NRIAG JOURNAL OF ASTRONOMY AND GEOPHYSICS
2019, VOL. 8, NO. 1, 34–44
https://doi.org/10.1080/20909977.2019.1615807

Taylor & Francis
Taylor & Francis Group

ARTICLE

Source mechanisms and simulation of ground motions of 18 and 22 July 2014 Suez earthquakes

Emad Kamal Mohamed

Department of Seismology, National Research Institute of Astronomy and Geophysics, Cairo, Egypt

ABSTRACT

On 18th and 22nd of July, 2014, two felt earthquakes have occurred in the northeastern part of Egypt (Cairo-Suez District) near Suez city with magnitude ML = 4.3 and ML = 4.0 respectively. The datasets used involves the two earthquakes recorded by Egyptian National Seismic Network (ENSN) and regional seismic stations (Jordan and Cyprus) to obtain the focal mechanism. A stochastic method is used to obtain high-frequency ground motion synthetics based on local site effect using 5 sites ambient noise (Microtremor) measurements to obtain the resonance frequency of the sediments. The ground motion parameters of (PGA), (PGV), (PGD) and spectral accelerations (SA) of the two earthquakes are obtained. The results show that the maximum value of the peak ground acceleration is observed at the site no. 1 (Northwest the apex of the Suez Gulf) due to near source-site distance and local site conditions (H/V = 4.4), while the minimum value is observed at the site no. 5 (Southwest of the small Bitter Lake) due to a large distance from the source (H/V = 2.10). The damped pseudo-acceleration was applied for the simulation at damping (0.5%, 1%, 5%, 10% and 20%). These results indicated, the efficiency and the importance of the local site conditions on strong ground motions.

KEYWORDS

Ground motions simulation; stochastic modelling; Cairo-Suez district; PGA; PGV; PGD; microtremor

1. Introduction

The northeastern part of Egypt (Cairo-Suez district zone) is characterized by small-to-moderate earthquakes due to the tectonic movement between African, Arabian and Eurasian plates. It has been affected by moderate-size historical earthquakes (e.g. 2200 BC, intensity = VII; macroseismic magnitude, MF = 5.4). The damaged earthquake occurred on October 1754 at the apex of the Gulf of Suez with intensity ranges VII–IX and MF = 6.6 (Ambraseys et al. 1994) and 1984 earthquake with M_W = 5.11 is located near Suez City (Abou El-Enean et al. 2010). Also, the 1st June 2013 Gulf of Suez earthquake has been studied by Toni (2017). The seismicity from 1900 to 2017 shows small-to-moderate earthquakes up to M_L = 5.

In the Cairo-Suez shear zone, two felt earthquakes were recorded by Egyptian National Seismic Network (ENSN) and some regional seismic stations from Jordan and Cyprus on 18th and 22nd July 2014 (Figure 1, Table 1). In the present study, the focal mechanisms of the two earthquakes are determined based on the first motion of P-waves polarities and the amplitude ratios of P, S_H and S_V-waves by using FOCMEC program (Snoke et al. 1984).

The study of the seismic wave propagation effects around active faults and near-surface field are important for understanding rock rheology, estimating seismic hazard, predicting future ground motions (Frankel et al. 2000), and designing geotechnical and structural engineering systems (NEHRP 2003). The site response plays important factor on modifications of seismic waves produced (variations in properties of materials) near the earth's surface from linear to non-linear if the amplitude of the wave is large enough (the associated dynamic stress), it would cause a change in the elastic property of the medium through the propagation path, and usually found in the highly fractured region, such as shallow sedimentary layers (Yu et al. 1992) and fault damage zones (Vidale and Li 2003). In general, it leads to larger motions on soil sites than on rock-like sites. Non-linear site effects are typically associated with strong ground motions (>100 Gal) (Beresnev and Wen 1996a) which are typically found in regions close to the epicenter of large earthquakes.

The ground motions parameter is necessary to design and evaluate structures and infrastructures under seismic hazard. However, the disaster of an earthquake depends on the following items: (i) Location of the epicenter, (ii) The earthquake's magnitude size, (iii) The source to site distance, (iv) The focal depth (deep earthquakes are less damaging than shallow earthquakes) and (v) Soil conditions; it acts as an important factor in influencing the damage level of an earthquake. The economic and social effects of earthquake disasters can be reduced by a comprehensive assessment of seismic hazard and risk in a particular area by (i) increasing the public awareness, (ii) upgrading the existing

CONTACT Emad Kamal Mohamed ekamal@nriag.sci.eg Department of Seismology, National Research Institute of Astronomy and Geophysics, Hewan, Cairo, Egypt

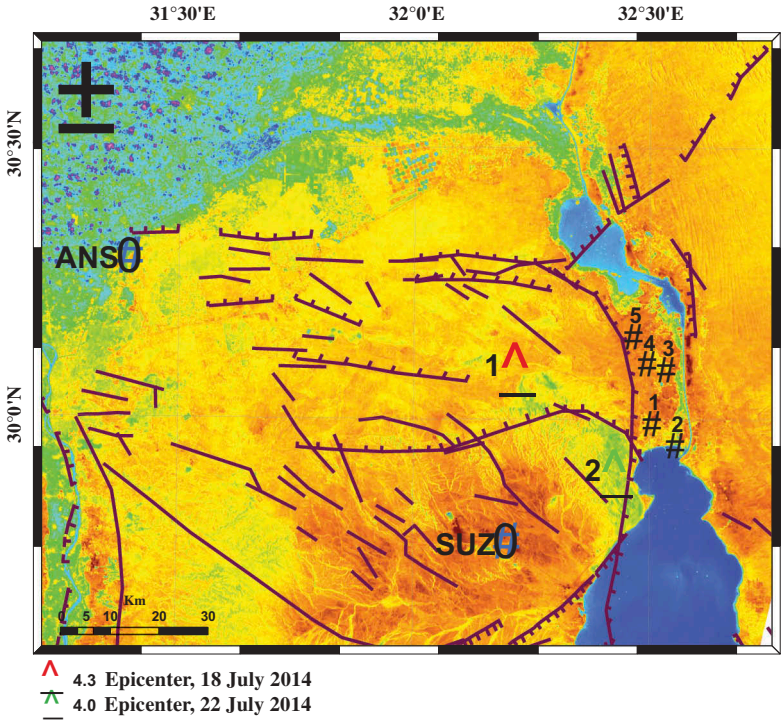

Figure 1. Landsat Image shows location map of the selected sites (1–5), Accelerograph stations (SUZ and ANS) and the epicenters (1,2) of the two earthquakes occurred on 18th and 22nd July 2014.

Table 1. Source parameters and focal mechanisms of the 18 and 22 July 2014 earthquakes.

			Location				
Source location	Date	Origin time (GMT)	Late.	Long.	Strike Dip Rake	Depth (Km)	M_L
NW Suez	18,072,014	20:01:29	30.10 °	32.24 °	26 71–23	21.3	4.3
SW Suez	22,072,014	03:03:44	29.92 °	32.44 °	341 71–23	30.4	4.0

buildings and engineering works and (iii) strong earthquake resistant designing for new strategic structures.

The topographic and sedimentary deposits can amplify ground motion. So, the amplification and the high level of damage are observed over soft soils and unconsolidated deposit than the consolidated and hard rocks.

The synthetic ground motion model becomes an alternative in the area which has a limited seismic record. This modelling helps seismologists to estimate the future hazard in the region by taking into account the local soil conditions. Increasing urbanization and construction of specific installations around the study area require a high sensitivity towards the public hazard caused by felt or damaging earthquakes.

The objectives of the present research are analyzing the available data of these earthquakes that occurred in Cairo-Suez district to provide an opportunity to study the present-day tectonics and stress pattern. In addition, the path and site effect is used to synthesize the horizontal shear wave ground motions. These parameters are very useful for assessment and mitigation of the seismic risk for high and significant constructions close to Cairo-Suez district zone (e.g. New Capital city)

2. Geologic and tectonic setting

Suez City is a part of the transitional zone between the Gulf of Suez rift and the unstable shelf of the northern part of Egypt (Omran 1989; Geriesh 1989). It is covered by sedimentary rocks belonging from the Cretaceous to Pleistocene and Holocene ages (Figure 2). The Cairo-Suez shear zone extends from the end of the Suez rift to the Nile Valley, through Ataqa Mountain and El-Galala El-Bahariya plateau. At Ataqa and Okheider Mountains, there is a succession of limestone related to Middle Eocene age lie at the northern part, while a succession of marl and coarse fossiliferous sandstone of Upper Eocene age is exposed at the southern low margins of Ataqa Mountain.

In the Cairo-Suez district, there are normal faults oriented NW–SE and rejuvenated E-ENE (Figure 1) formed by dextral transtension of Miocene and post-Miocene extension due to the rift of Arabia away from Africa (Moustafa et al. 1998). The throw of the faults in the northern part of the Miocene rift was transferred into the Cairo-Suez district (Moustafa and Abd-Allah 1992) through the deep-seated E-Woriented faults while the Early Miocene deformation was associated with basaltic volcanicity (Meneisy 1990).

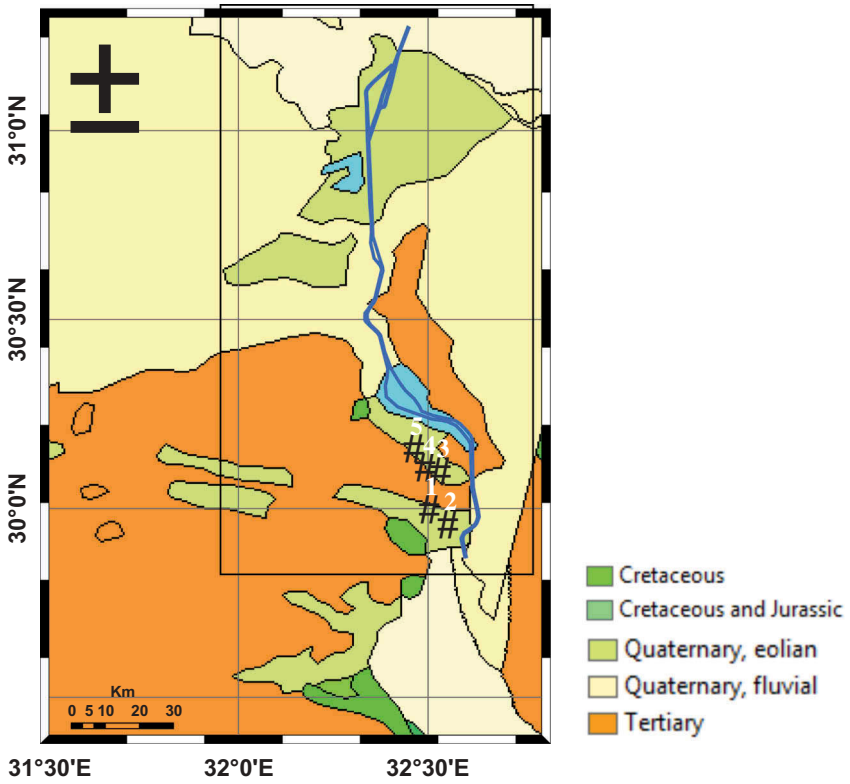

Figure 2. Geologic map of the study area and studied sites (Black triangles) (modified from the US. Geological Survey's World Energy Project 1997–2000).

3. Seismicity

The Cairo-Suez district zone occupies the northeastern part of Egypt; it is characterized by small-to-moderate earthquakes (Figure 3). This seismic activity reveals the tectonic framework and the type of crustal deformation in that area. The historical earthquakes in this region showed few moderate to large size events (e.g. 2200 BC (intensity = VII; macroseismic magnitude, MF = 5.4), the destructive earthquake occurred on October 1754 at the apex of the Gulf of Suez with intensity ranges VII–IX and MF = 6.6 (Ambraseys et al. 1994) and 1984 earthquake (M_W = 5.11) is located near Suez City (Abou El-Enean et al. 2010). The recent seismicity from 1900 to 2017 shows small-to-few-moderate earthquakes up to M_L = 5 are observed. Most of the activity is clustered over the Gulf of Suez at its extension towards north overlaying the NW and E-W faults that affect this active part of the Eastern Desert,

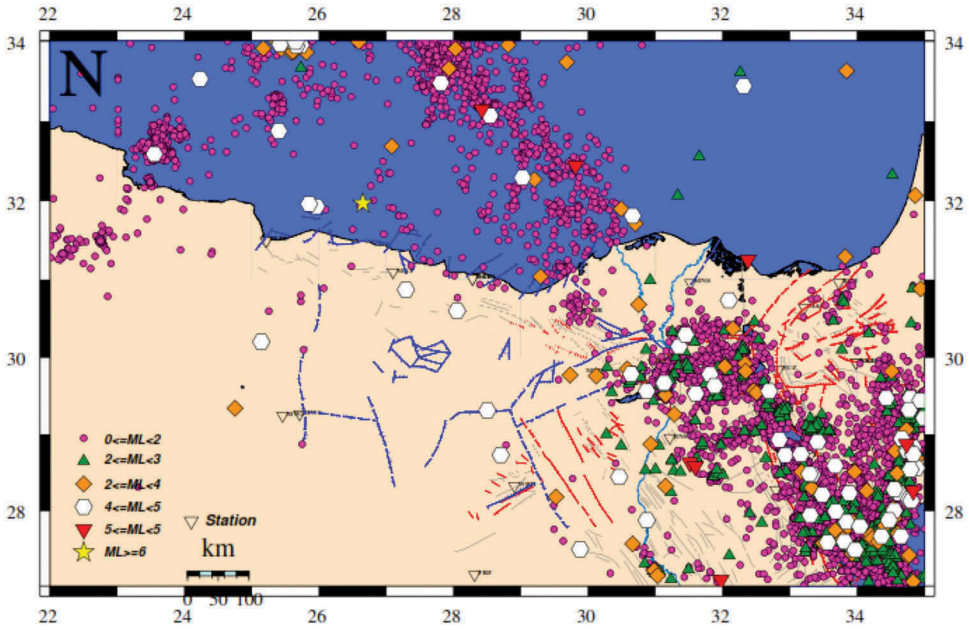

Figure 3. Seismicity map of northern Egypt recorded by ENSN and regional networks during the period from November 1997 to December 2016 (ENSN Bulletin 2014), Red lines represent the recent surface faults.

4. Datasets and methodology

The datasets used in the present study involves the seismic recording of the two earthquakes by (ENSN) and some regional seismic stations from neighbouring seismic networks from Jordan and Cyprus. The hypocentral parameters are determined using a dataset of 27 seismograms (Figure 4) based on the linearized inversion program, HYPOCENTER 3.2 (Lienert et al. 1986; Lienert and Havskov 1995; Havskov and Ottemoller 1999; Havskov and Ottemöller 2014) under SEISAN software. The crustal velocity model that suggested by Makris et al. (1979) is used for this study. The fault plane solutions of the 18th and 22nd July 2014 earthquakes is obtained by using P-wave first motion polarities and the amplitude ratios of P-wave, S_H-wave and S_V-wave with FOCMEC program (Snoke et al. 1984).

In the present work, the point-source of Stochastic Method is used to generate high-frequency ground motion synthetics for Suez earthquakes based on local site effect using 5 sites microtremor measurements around Suez City considering the sources and the paths (Figure 1). This method assumes that the source is concentrated at a point and the acceleration time series which generated will carry both deterministic and random aspects of ground motion shaking.

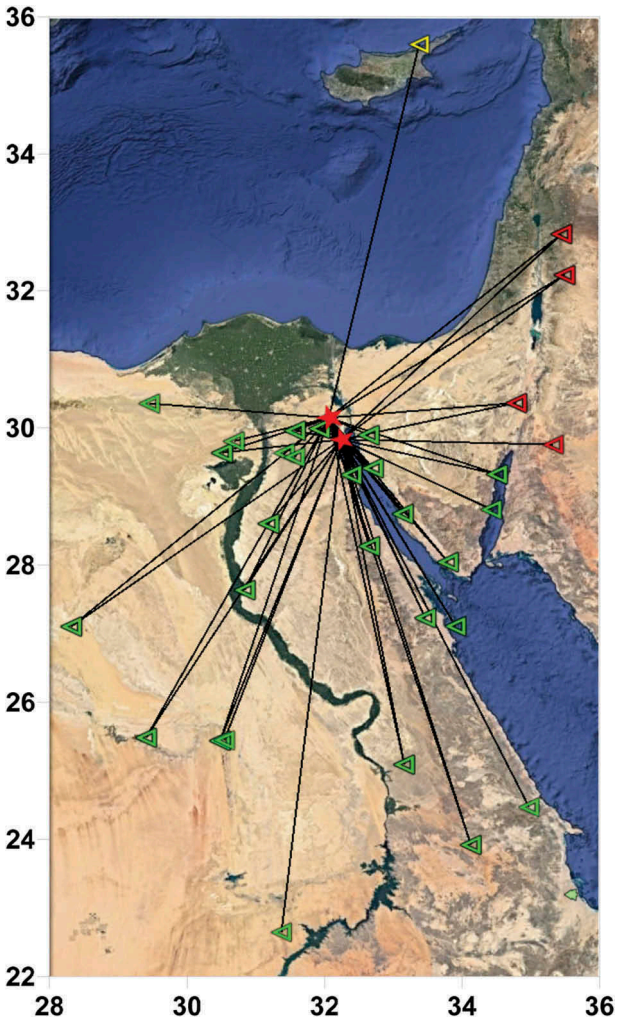

Figure 4. Location map showing the epicenter of 18th and 22nd July 2014 earthquakes (Red stars), Seismic (ENSN) stations (Green triangles); Regional stations of Jordan and Cyprus (Red and Yellow triangles).

A stochastic time-domain simulation method is employed by (Boore 2003) and used as a general equation from random process theory. The total spectra of the ground motion at a site will contribute from the seismic source, the path and the site. Andrews (1986) stated that the shear wave spectrum (point source spectrum) Y (f), for the source (i) and site (j) is decomposed as:

$$Yij(f) = Ei(f) \,.\, Pij(f) \,.\, Gj(f) \qquad (4\text{-}1)$$

whereas, E (*f*) the source spectrum, P (*f*) the path spectrum effect (geometrical spreading and attenuation) and G (*f*) the site spectrum (amplification or de-amplification).

The path spectrum is represented by the geometrical spreading and whole-path attenuation Q (f) as:

$$P(f) = r^{-y} e^{(-ft)/Q(f)} \qquad (4\text{-}2)$$

whereas, (y) is set to 1.0, consistent with body waves in the uniform medium, (*t*) is the travel time, (*r*) is the hypocentral distance.

The method begins, with the specification of the furrier amplitude spectrum of ground acceleration as a function of earthquake size (moment magnitude), distance and frequency Y (Mo, R, f), which can be represented as.

$$Y(M_o, R, f) = \mathrm{E}(M_o, f)\,\mathrm{P}(R, f)\,\mathrm{G}(f) I(f) \qquad (4\text{-}3)$$

The Fourier spectrum of ground motion is a critical parameter for peak motions decrease with increasing duration (Boore 2003). The duration is a function of the path, as well as the source using this equation;

$$T = To + bR \qquad (4\text{-}4)$$

whereas, (*To*) is the source duration, and (*bR*) represents the path relative term that accounts for dispersion. Following Hanks and McGuire (1981), the source duration is related to the corner frequency as:

$$\mathrm{T_o} = f\mathrm{c}^{-1} \qquad (4\text{-}5)$$

5. Fault plane solutions

The digital waveform data of the 18th and 22nd July 2014 earthquakes were extracted from the ENSN and some regional seismic stations from Jordan and Cyprus networks. The regional seismic station's data is used to reduce the azimuthal gap of the station's coverage for obtaining the best solution of the focal mechanism (Figure 4). The source parameters andmechanism of these events are presented in Table 1. The fault plane solutions show normal faults with strike-slip components trending NE-SW to NW-SE and NW-SE to E-W for 18th and 22nd July earthquakes, respectively (Figure

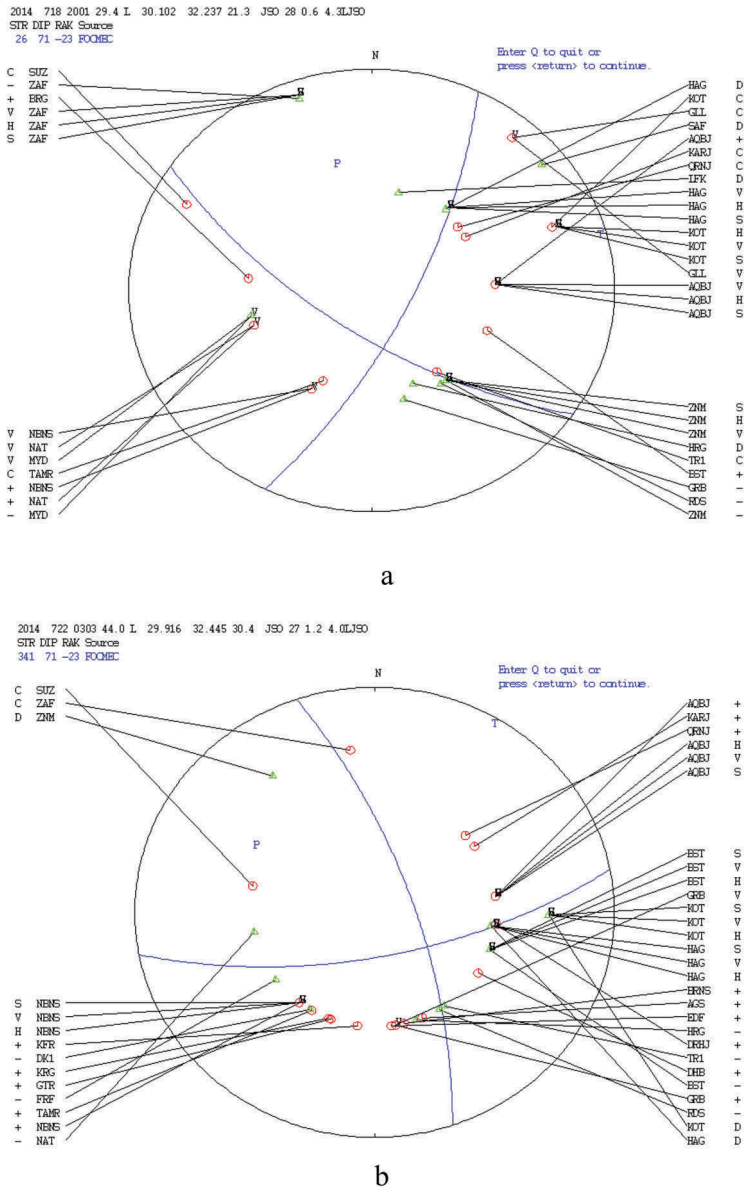

Figure 5. Fault plane solutions of the 18 July 2014 (up) and the 22 July 2014 (down) earthquakes based on the polarities and amplitude ratios.

5a, 5b). These results reflect a good agreement with the surface faults crossing the Eastern Desert from the apex of the Gulf of Suez towards Cairo in the East-West direction and compatible with the main trend of the Suez Gulf. The source parameters and mechanism of these events are presented in.

6. The simulation of ground motions

Ground Motion Prediction Equations (GMPEs) provide measures of the ground motions, such as standard deviation, pseudo-spectral velocity (PSV), the peak ground acceleration and the peak ground velocity. These parameters are used to represent the response of the simple structures to ground-shaking e.g. residential buildings; therefore, it provides useful input for engineering applications. The damping and periods have a significant impact on the response (Bommer and Alarcón 2006).

The ground motion parameters of peak ground acceleration, peak ground velocity, peak ground displacement and response spectra/pseudo-spectral acceleration (PSA) are obtained from empirical attenuation equations that relate to the magnitude of the earthquake, the source–site distance, and the site condition. The stochastic method of Boore (2003) with the site-dependent spectral model is used for this study based on the models of radiated spectra, and the semi-empirical modelling of the site response. The data of the site response used in this study is taken from the previous study (Mohamed et al. 2016) using ambient noise (microtremor) data of 5 sites.

7. Results and discussion

In the present study, the output of HVSR curves of the fundamental frequency (f_o) and amplitude

Table 2. The epicentral distances from each site to the seismic sources.

Date of the Source	Dis. (Km) The site 1	Dis. (Km) The site 2	Dis. (Km) The site 3	Dis. (Km) The site 4	Dis. (Km) The site 5
18,072,014	28.37	35.24	29.79	25.69	23
22,072,014	11.07	12.64	21.96	21.40	25.78

Table 3. The simulated PGA values at the selected sites for the two studied earthquakes.

Site No.	Lat.	Long.	f_o (Hz)	H/V (A_o)	PGA (cm/s^2) Source 1	PGA (cm/s^2) Source 2
1	29.99	32.51	0.58	4.4	9.604E+00	34.03E+00
2	29.95	32.56	0.58	3.12	4.499E+00	18.83E+00
3	30.09	32.54	0.60	3.15	6.332E+00	6.987E+00
4	30.10	32.50	0.60	3.92	8.350E+00	7.519E+00
5	30.15	32.47	0.60	2.10	6.689E+00	3.517E+00

ratios (A_o), moment magnitude, and the seismic source distance to each site represent the input parameters of SMSIM Program (Boore 1996). The analysis gives response spectra and pseudo-spectral acceleration at different damping for each site.

The spectral ratio is used to analyze temporal changes in site response associated with the strong ground motion for the two earthquakes occurred on 18th and 22nd July 2014 (source 1, and source 2 respectively). The influence of magnitude, epicentral distances and site conditions on ground motion are displayed. The influence of the distance from the site to the source and local site conditions for the data recorded from the two earthquakes (e.g. PGA at sites 1 (34 cm/s^2) and 5 (3.5 cm/s^2) from 22 July

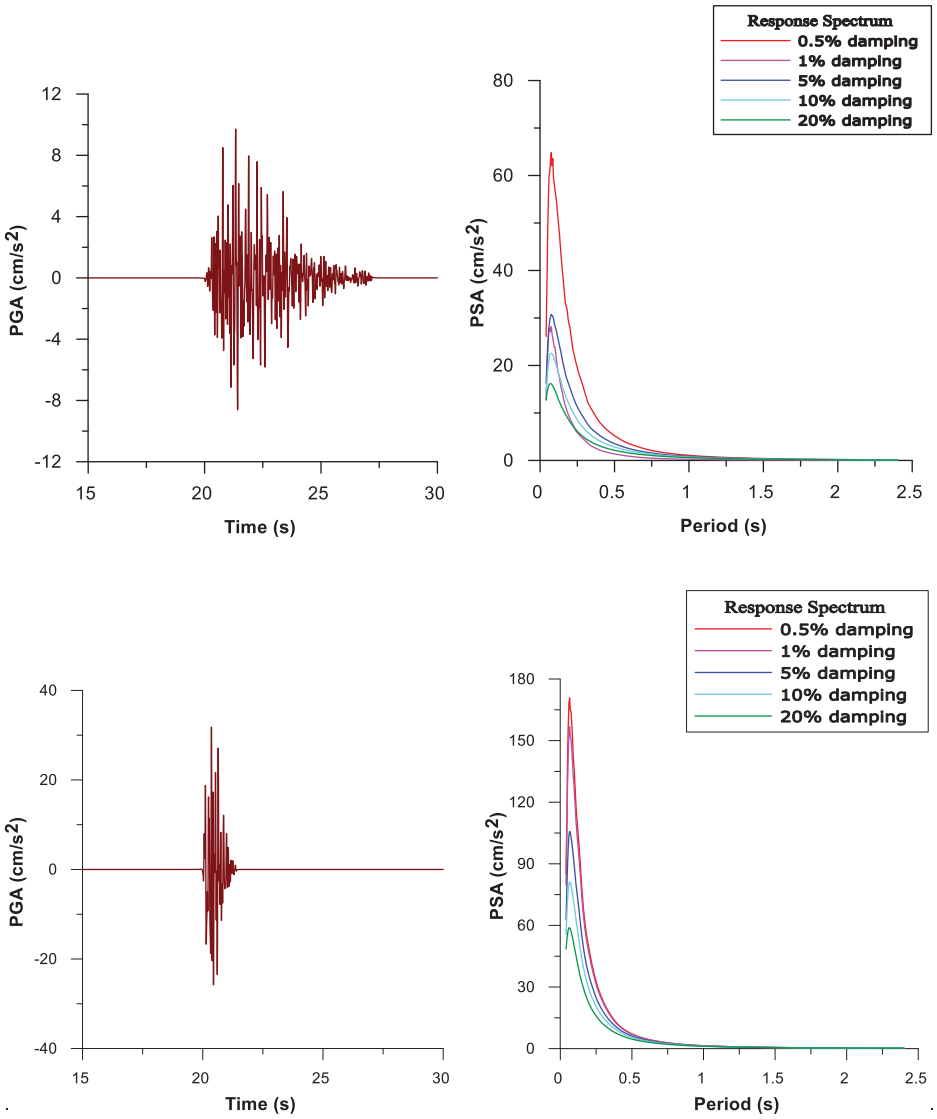

Figure 6. The simulated acceleration (left) and pseudo-spectral acceleration (right) from seismic source 1 (up) and seismic source 2 (down) at the site no. 1 (A_0 = 4.4).

earthquake) and (PGA at sites 1 (9.6 cm/s^2) and 2 (4.49 cm/s^2) from 18th July earthquake). The epicentral distances from each site to the seismic sources are listed in Table 2. The simulated PGA values at the selected sites (1, 2, 3, 4 and 5) are shown in Table 3.

The peak ground acceleration and the response spectra at different damping (0.5%, 1%, 5%, 10% and 20%) of pseudo-spectral acceleration were simulated for the two earthquakes on the sites having different amplification values (Figs. 6 and 11).

The integration of ground motion parameters for seismic source 1 and seismic source 2 at the same site no. 1 is shown in Figure 7 it indicated that the ground motion simulation of seismic source 2 is very high than seismic source 1 due

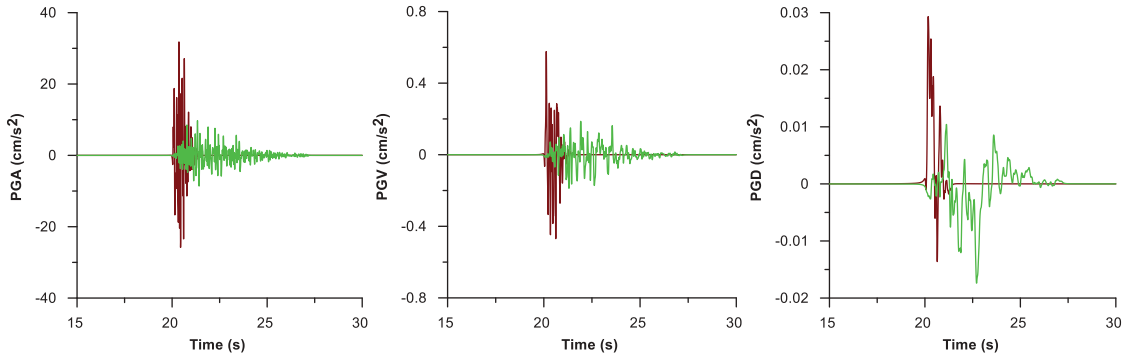

Figure 7. Integration of ground motion parameters for seismic source 1 (Green) and seismic source 2 (Dark Red) at the same site no. 1.

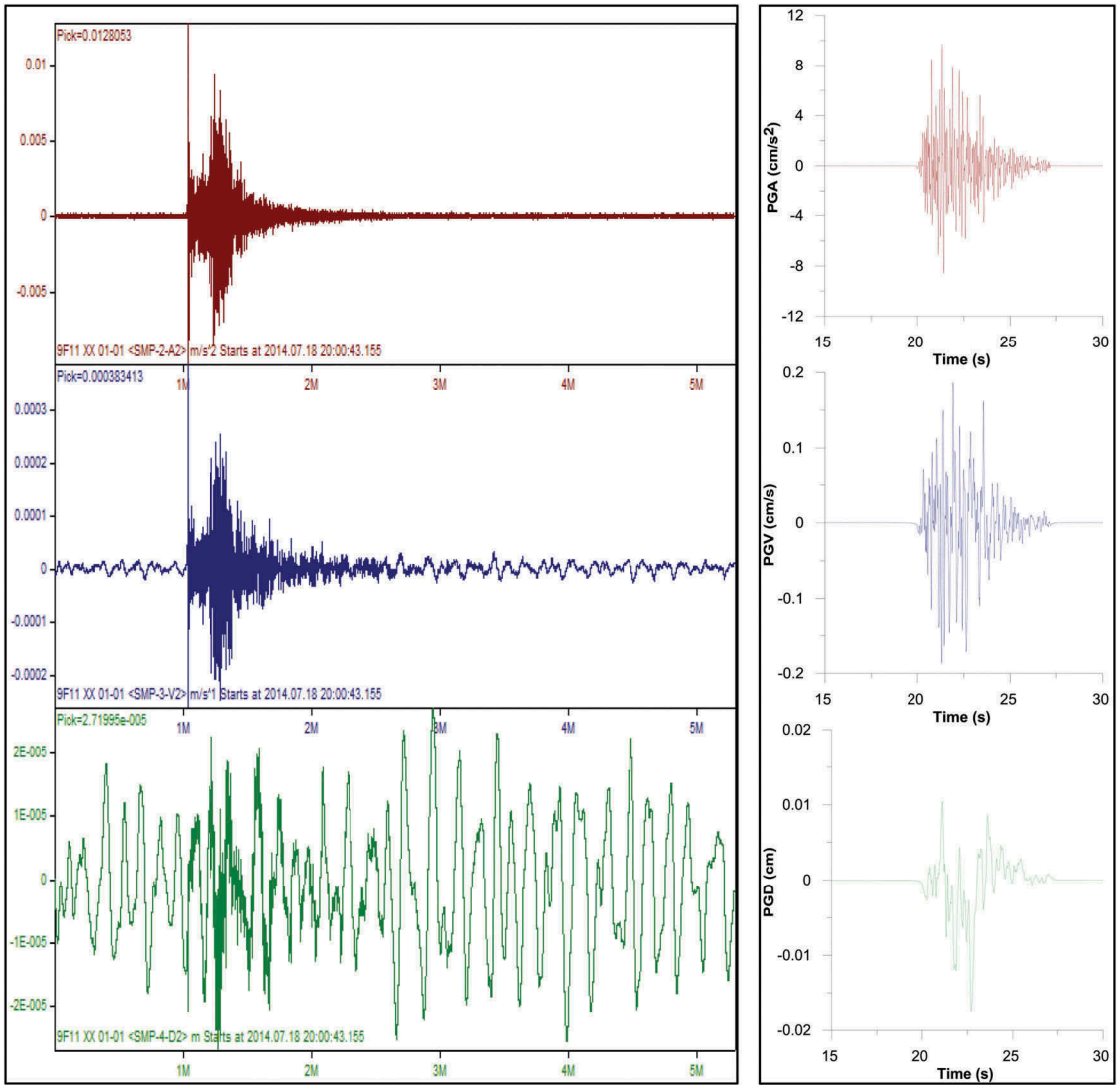

Figure 8. Comparison between recorded (PGA, PGV, PGD) (left panel) at ANS Accelerograph station, and simulated acceleration, velocity and, displacement time series from the epicenter of 18 July 2014 earthquake at the site no. 1.

to small distance (11 km) from the source to the site.

Figure (8) shows comparison between recorded time series at ANS accelerograph station (83 km from the epicenter) and the simulated shear wave acceleration, velocity and displacement time series at the site no. 1 for seismic source 1. The results indicate that the low value of PGA (1.5 cm/s2) is observed at ANS station due to a large distance from the source to the site.

Figure (9) shows a comparison between recorded time series at SUZ accelerograph station (37.5 km from the epicenter) and the simulated shear wave acceleration, velocity and, displacement time series at the site no. 1 from seismic source 1. The value of PGA at the site 1 equal 9.6 cm/s2 while the observed acceleration equal 11.8 cm/s2.

Figure 10 shows a comparison between recorded time series at SUZ accelerograph station (28 km from the epicenter) and simulated shear wave acceleration, velocity and, displacement time series from seismic source 2 at the site no. 1. The simulated PGA equal 34.03 cm/s^2 and the observed PGA = 11.1 cm/s^2. These results indicate that the high PGA value is related to the effect of local site condition and the source- site distance.

The integration of ground motion parameters for seismic source 1 and seismic source 2 at the same site no. 2 is shown in Figure 11; it indicated that the ground motion simulation of seismic source 2 is very high than seismic source 1 due to small distance (12.64 km) from the source to the site.

The integration of ground motion parameters for seismic source 1 and seismic source 2 at the others sites 2, 3 and 4 reflect clearly the effect distance and site amplification on the calculated PGA. Also, when the distances from the sources become closer to each other, the calculated PGA showed closer values.

8. Conclusion

Two moderate felt earthquakes have occurred on 18th and 22nd July 2014 in Cairo-Suez shear zone and recorded by Egyptian National Seismic Network (ENSN) and some regional seismic

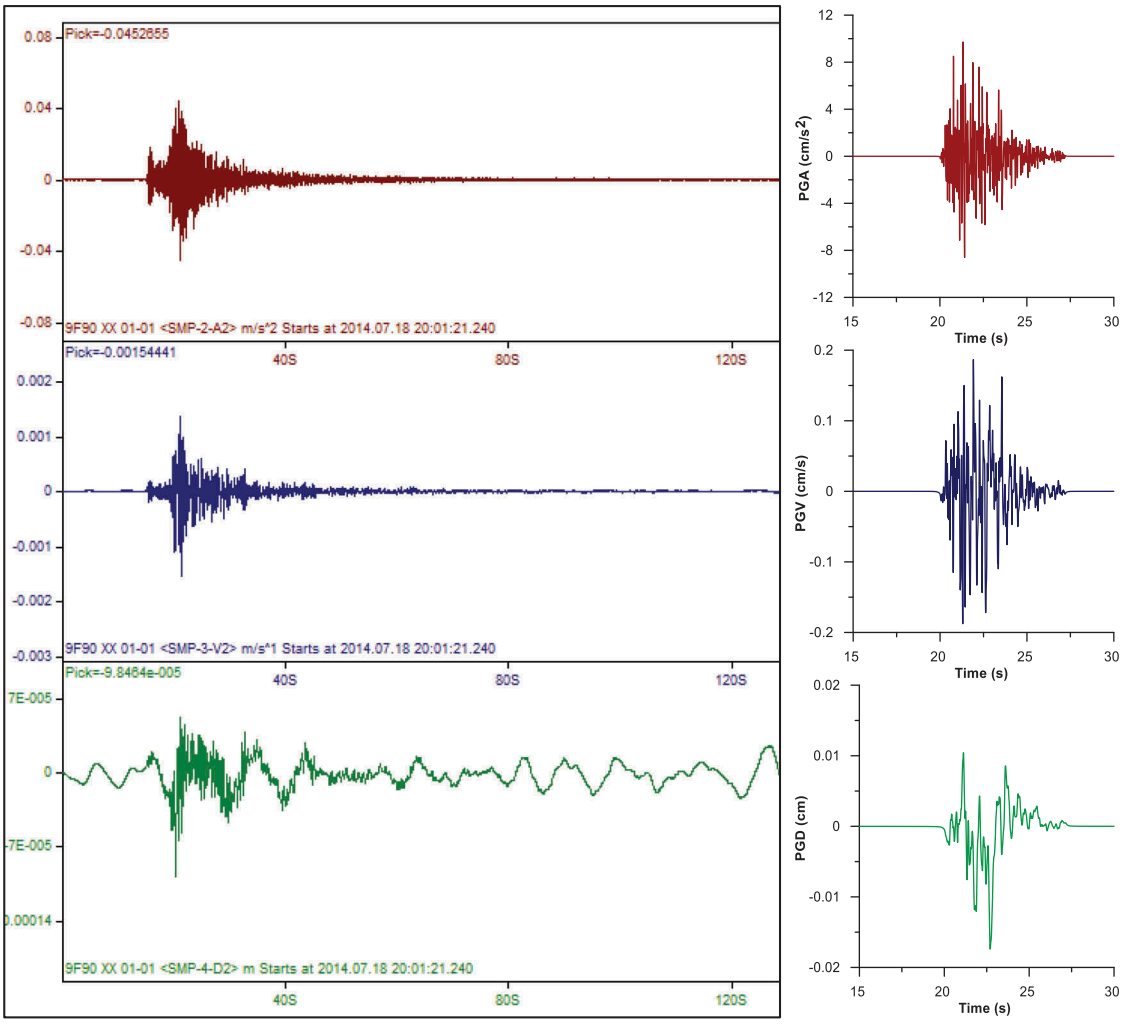

Figure 9. Comparison between recorded (left panel) and simulated (right panel) acceleration, velocity and, displacement time series at SUZ Accelerograph station for 18 July 2014 earthquake at the site no. 1.

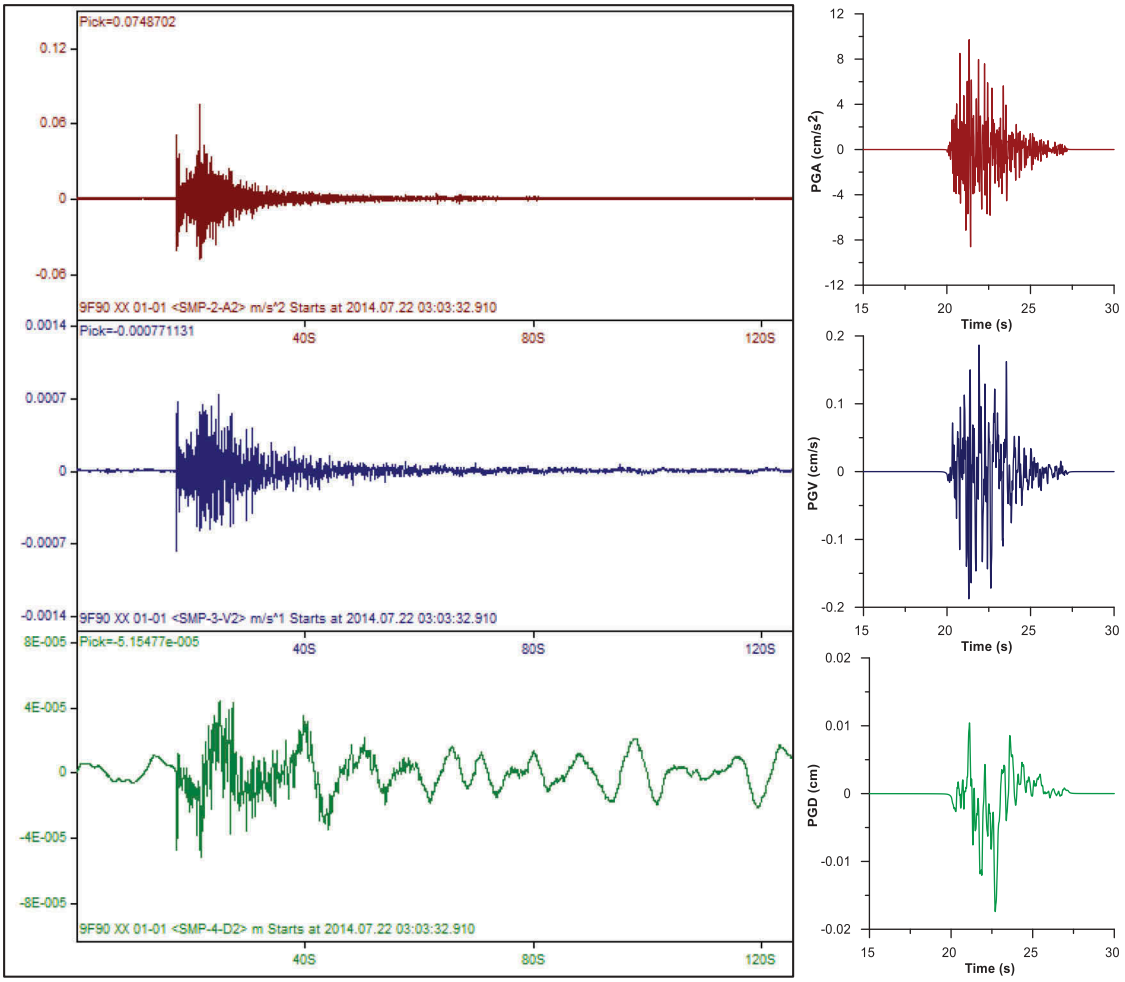

Figure 10. Comparison between recorded (left panel) and simulated (right panel) acceleration, velocity and, displacement time series at SUZ Accelerograph station for 22 July 2014 earthquake at the site no. 1.

stations from Jordan and Cyprus to obtain the focal mechanism. The regional stations are used to reduce the azimuthal gap of the station's coverage. The focal mechanism of the two earthquakes carried out based on the first motion of P-waves and the amplitude ratios using FOCMEC program under SEISAN software show normal faults with strike-slip components trending NE-SW to NW-SE and NW-SE to E-W for 18th and 22nd July earthquakes, respectively (Figure 5). These results are compatible with the trends of the Gulf of Suez and Cairo Suez shear zone.

The results of ground motion simulation for 18th July earthquake indicate that the maximum peak ground acceleration observed at site 1 is 9.6 cm/s^2 (28 Km, A_o = 4.4) and the minimum value calculated at site 2 (4.49 cm/s^2 at large distance 35 km). While the maximum value of ground motions from 22nd July earthquake at site 1 is 34 cm/s^2 (11 km) and the minimum value at site 5 is 3.5 cm/s^2 (25 Km). The variations are related to the influence of local site conditions and source-to-site distance, respectively. Based on ground motion and sites studies, high values of amplification factors play a significant role in seismic disasters. Therefore, the influence of the site is important to mitigate the seismic risk and should be taken into account during the design of strategic constructions.

In this study, the peak ground acceleration (PGA) is restricted as the most interesting parameter in civil engineering applications. The PGA is easy to measure because the response of most instruments is proportional to ground acceleration. It can be related to the force on short-period buildings and single stations available numbers to enable rough evaluation of the importance of records. The results are compatible with the geologic features of the selected sites as is shown in the geologic map of the study area (Figure 3), whereas the sites 1 and 2 located at quaternary aeolian sand deposits which responsible for the amplification of the seismic ground motion in the study area.

These results are very useful for civil engineers to study the response of both short-period and long-period structures; therefore, it can be used to estimate the safety of the existing buildings and engineering works by making necessary upgrading or making strong earthquakes resistant design for new important structures.

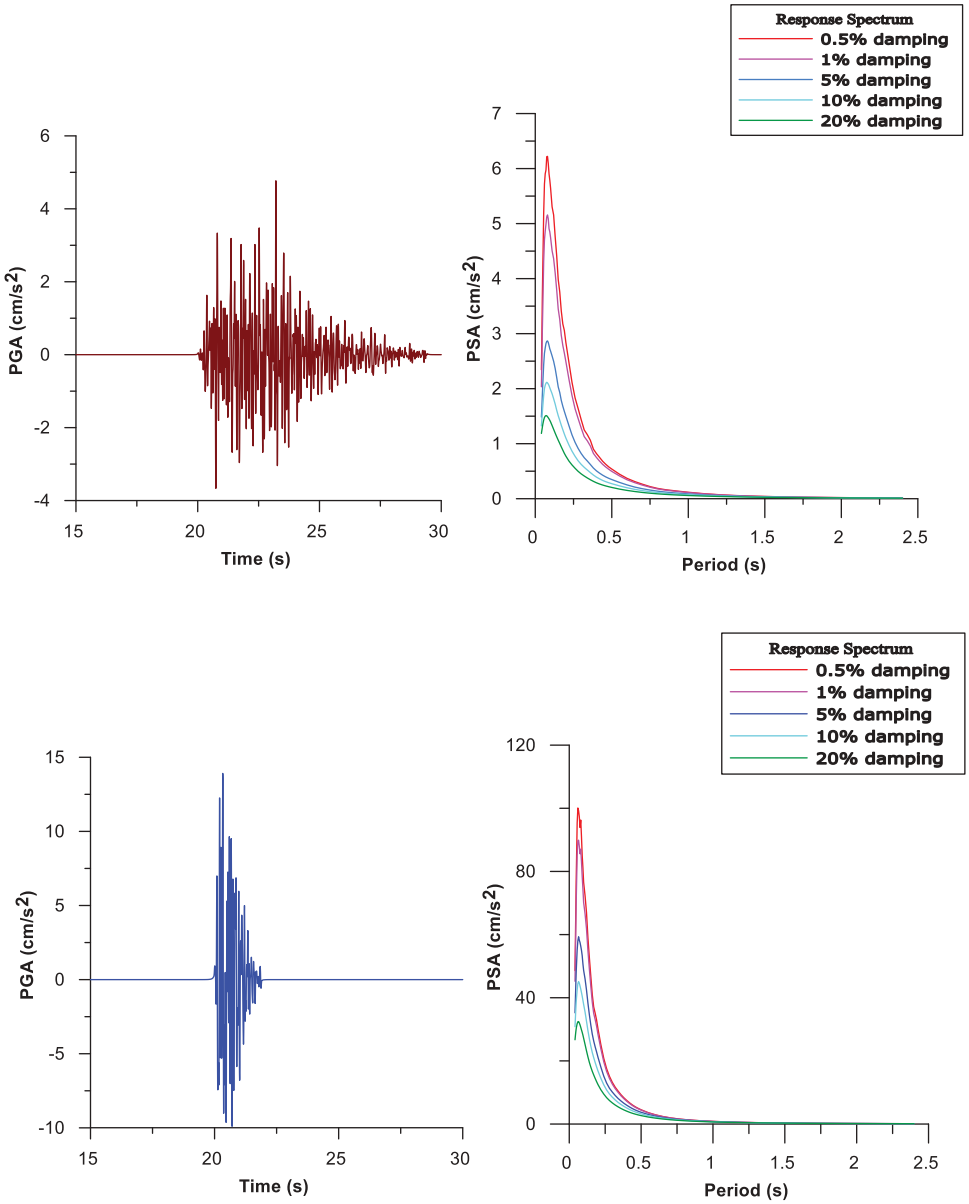

Figure 11. The simulated acceleration (left) and pseudo-spectral acceleration (right) from seismic source 1 (up) and seismic source 2 (down) at site 2 (A_0 = 3.12).

Acknowledgements

I would like to thank the Egyptian Seismological Network and Observatories & Research Facilities for European Seismology (ORFEUS) for providing the data for this analysis. Also, I wish to thank the editor and reviewers for time and efforts to review this work and for their constructive suggestions.

Disclosure statement

No potential conflict of interest was reported by the author.

References

Abou El-Enean KM, Mohamed AE, Hussein HM. 2010. Source parameters and ground motion of the Suez-Cairo shear zone earthquakes, Eastern Desert, Egypt. Nat. Hazards. 52:431–451. doi:10.1007/s11069-009-9388-x

Ambraseys NN, Melville CP, Adams RD. 1994. The seismicity of Egypt, Arabia and the Red Sea. Cambridge: Cambridge University Press; p. 182.

Andrews DJ. 1986. Objective determination of source parameters and similarity of earthquakes of different sizes. In: Das JB, Scholz CH, editors. Earthquake Source Mechanics. Washington (DC): AGU; p. 259–268.

Beresnev I, Wen K. 1996a. Nonlinear soil response-A reality? Bull Seism Soc Am. 86:1964–1978.

Bommer JJ, Alarcón JE. 2006. The prediction and use of peak ground velocity. J Earthq Eng. 10(1):1–31.

Boore DM 1996: SMSIM–fortran programs for simulating ground motions from earthquakes: version 1.0, U.S. Geol. Surv., Open-File Report. 96-80-A and 96-80-B, 73 pp.

Boore DM. 2003. Simulation of ground motion using the stochastic method; Seismic motion, lithospheric structures, earthquake and volcanic sources; the Keiiti Aki volume. Pure Appl Geophys. 160:635–676.

ENSN Bulletin. 2014. Egyptian National Seismic Network, Earthquakes in and around Egypt. Egypt:National Research Institute of Astronomy and Geophysics.

Frankel A, Mueller C, Barnhard T, Leyendecker E, Wesson R, Harmsen S, Klein F, Perkins D, Dickman N, Hanson S. 2000. USGS National Seismic Hazard Maps. Earthq Spectra. 16:1–19.

Geriesh H, 1989. Hydrogeological Investigations of West Ismailia Area, Egypt, M.Sc. Thesis, Faculty of Science, Suez Canal University, Ismailia, 210 p.

Hanks TC, McGuire RK. 1981. The character of high-frequency strong ground motion Bull. Seism Soc Am. 71:2071–2095.

Havskov J, Ottemoller L. 1999. SeisAn Earthquake analysis software. Seis Res Lett. 70:1999. http://www.seismosoc.org/publications/SRL/SRL_70/srl_70-5_es.html.

Havskov J, Ottemöller L. 2014. Routine Data Processing in Earthquake Seismology with Sample Data. Exercis Software Sep. 2014. Springer. http://www.springer.com/earth+sciences+and+geography/geophysics/book/978-90-481-8696-9.

Lienert BRE, Berg E, Frazer LN. 1986. Hypocenter: an earthquake location method using centred, scaled, and adaptively least squares. Bull Seismol Soc Am. 76:771–783.

Lienert BRE, Havskov J. 1995. A computer program for locating earthquakes both locally and globally. Seismol Res Lett. 66:26–36.

Makris J, Stofen B, Vees R, Allam A, Maamoun M, Shehata W (1979) Deep seismic sounding in Egypt. Part I: the Mediterranean Sea between Crete- Sidi Barani and the coastal area of Egypt. Unpublished report, National Research Institute of Astronomy and Geophysics, Helwan (Egypt)

Meneisy MY. 1990. Volcanicity. In: Said R, Balkema AA, editors. The geology of Egypt, Chapter 9. Netherlands: Rotterdam; p. 157–172.

Mohamed EK, Shokry MMF, Hassoup A, Helal AMA. 2016. Evaluation of local site effect in the western side of the Suez Canal area by applying H/V and MASW techniques. J Afr Earth Sci. 123:403–419.

Moustafa A, Abd-Allah A. 1992. Transfer zones with en echelon faulting at the northern end of the Suez rift. Tectonics. 11(3):499–509. doi:10.1029/91TC03184.

Moustafa A, El-Badrawy R, Gibali H, 1998. Pervasive E-ENE oriented faults in northern Egypt and their effect on the Development and inversion of prolific sedimentary basis. Proceedings of 14th petroleum conference, Egypt, vol 1. Egyptian General Petroleum Corporation, pp 51–67.

NEHRP, 2003. NEHRP recommended provisions for seismic regulations for new buildings and other structures, Part 1: Provisions, Building Seismic Safety Council, Washington (DC, USA). Charles Thornton, FEMA P-450

Omran M, 1989. Geological Studies of Shabraweet Area, Suez Canal, Egypt, M.Sc. Thesis, Faculty of Science, Suez Canal University, Ismailia, 135 p.

Snoke JA, Munsey JW, Teague AG, Bollinger GA. 1984. A program for focal mechanism determination by combined use of polarity and SV-P amplitude ratio data. Earthq Note. 55:15.

Toni M. 2017. Simulation of strong ground motion parameters of the 1 June 2013 Gulf of Suez earthquake, Egypt. NRIAG J Astron Geophys. 6:30–40. doi:10.1016/j.nrjag.2016.12.002

Vidale J, Li Y. 2003. Damage to the shallow Landers fault from the nearby Hector Mine earthquake. Nature. 421:524–526.

Yu G, Anderson J, Siddharthan R. 1992. On the characteristics of nonlinear soil response. Bull Seism Soc Am. 83:218–244.